

Laser operation of Yb^{3+} in the acentric RbTiOPO_4 codoped with Nb^{5+}

Xavier Mateos,^{1,*} Valentin Petrov,¹ Alexandra Peña,² Joan J. Carvajal,² Magdalena Aguiló,² Francesc Díaz,² Patricia Segonds,³ and Benoît Boulanger³

¹Max-Born-Institute for Nonlinear Optics and Ultrafast Spectroscopy, 2A Max-Born-Strasse, D-12489 Berlin, Germany

²Física i Cristallografia de Materials, Universitat Rovira i Virgili, Campus Sescelades, Calle Marcellí Domingo, E-43007 Tarragona, Spain

³Institut Néel/CNRS—UJF, BP 166, F-38042 Grenoble Cedex 9, France

*Corresponding author: mateos@mbi-berlin.de

Received February 20, 2007; revised May 3, 2007; accepted May 3, 2007; posted May 11, 2007 (Doc. ID 80195); published xx xx, xxxx

We report on continuous-wave lasing of Yb^{3+} at room temperature in the noncentrosymmetric RbTiOPO_4 crystal, codoped with Nb, for all three possible polarizations. A maximum output power of 154 mW at 1050 nm was obtained for an absorbed power of 386 mW. The highest slope efficiency reached $\approx 60\%$ and the lowest threshold (with respect to the absorbed power) was 18 mW. The laser was tunable from 1009 to 1081 nm. © 2007 Optical Society of America
OCIS codes: 140.5680, 140.3380, 160.4330, 160.5690.

Self-frequency doubling (SFD) crystals, which convert the fundamental emission to the second harmonic, are important for the development of compact and efficient laser sources in the visible. In the past, the major part of the SFD studies was devoted to the ${}^4\text{F}_{3/2} \rightarrow {}^4\text{I}_{11/2}$ transition of the Nd^{3+} ion [1]. The Yb^{3+} ion that operates in the same 1 μm spectral range as a quasi-three-level system on the single ${}^2\text{F}_{5/2} \rightarrow {}^2\text{F}_{7/2}$ transition has a number of advantages including (1) low quantum defect when pumped by InGaAs diodes, i.e., less thermal load; (2) broad absorption bandwidth, i.e., less critical pump wavelength; (3) broad emission bandwidth that allows larger tunability and generation of ultrashort laser pulses; (4) longer lifetime; and (5) absence of undesirable processes such as excited state absorption, upconversion, and nonradiative interaction among excited states. The last advantage is especially relevant to SFD because using Yb allows one to avoid absorption losses at the second harmonic.

So far, lasing of Yb^{3+} has been demonstrated only in six acentric hosts, $\text{XAl}_3(\text{BO}_3)_4$ [2,3] and $\text{XC}_2\text{O}(\text{BO}_3)_3$ [4,5], where $\text{X}=\text{Y}$ or Gd , LiNbO_3 [6], and $\text{KGd}(\text{PO}_3)_4$ [7]. The KTiOPO_4 (KTP) family of nonlinear optical crystals (orthorhombic, biaxial crystals belonging to the non-centrosymmetric space group $Pna2_1$ -point group $mm2$) are well-known materials for frequency conversion, in particular for frequency doubling of Nd lasers, with mature growth technology, high nonlinearity, and damage threshold, and they can be poled by electric field to obtain quasi-phase-matching. However, the doping of KTP with trivalent lanthanide ions turned out to be a great challenge and the maximum levels previously achieved for bulk crystals did not exceed a level ranging between 5×10^{17} and $6 \times 10^{18} \text{ cm}^{-3}$, which is too low for laser operation. Recently, on the basis of charge compensation and codoping with Nb^{5+} , the isostructural RbTiOPO_4 (RTP) was successfully doped with Yb up to $\approx 2 \times 10^{20} \text{ cm}^{-3}$ (2.2 at.%), pre-

serving the value of the effective nonlinearity [8]. Moreover, the large Stark splitting of the ground state of Yb in Nb:RTP (955 cm^{-1}) [8] results in a rather low (0.76%) population of the highest ${}^2\text{F}_{7/2}$ sublevel at room temperature. In the present letter, we report on efficient laser operation of Yb:Nb:RTP, end-pumped by a Ti:sapphire laser. This is, to the best of our knowledge, the first realization of laser generation of Yb in a nonlinear crystal belonging to the KTP family. We analyze the polarization dependence and demonstrate extremely broad tunability with a FWHM of 59 nm.

The single crystal of Yb:Nb:RTP used in the present study was grown by a high temperature solution growth method: top-seeded solution growth with slow cooling in a vertical tubular furnace [9]. The solution was prepared by mixing the initial reagents Rb_2CO_3 (99%), $\text{NH}_4\text{H}_2\text{PO}_4$ (99%), TiO_2 (99.9%), Nb_2O_5 (99.9%), and Yb_2O_3 (99.9%) in a 125 cm^3 Pt crucible. The mixture was then heated until total bubbling of NH_3 , H_2O , and CO_2 , and homogenization of the solution were achieved. The seed used was very thick along the a -axis because when doping RTP with Nb^{5+} the crystals show a plate-like habit, and the only way to increase the dimension along the aforementioned direction is using that kind of seed. The crystallographic c -axis of the seed was perpendicular to the surface of the solution, the a -axis was always radial with respect to the rotation, and the seed was offset by $\approx 5 \text{ mm}$ from the rotation axis. Moreover, to facilitate the stirring of the solution, the seed was attached to a special growth device (see [9]), consisting of a Pt turbine rotating together with the crystal seed at 80 rpm. Prior to the crystal growth, the saturation temperature (T_S) was measured by examining the growth and dissolution of the seed. The grown crystals were slowly removed from the solution and kept inside the furnace while cooling it down to room temperature (at 15 K/h) to avoid any thermal stress.

Table 1 shows the relation between the seed size and the obtained crystal size in the a direction. All crystals were grown in a solution with composition $\text{Rb}_2\text{O}-\text{P}_2\text{O}_5-(\text{TiO}_2+\text{Nb}_2\text{O}_5+\text{Yb}_2\text{O}_3)=40.8-27.2-(30.4-0.96-0.64)$ mol% and a weight of 159g. By comparing the first two experiments, as the seed width increases the crystal size also increases, and so does the crystal weight. In the third experiment, although the seed width was similar, the crystal obtained was smaller than the one obtained in the previous experiment. This was because of the shorter growth time (faster growth rate). Finally, by increasing the cooling interval in the slowest part of the cooling process, we obtained growth conditions that resulted in the larger crystal shown in Fig. 1 from which the sample used for the present laser experiment was extracted.

The laser setup is shown in Fig. 2. The pump beam from a homemade Ti:sapphire laser (FWHM < 1 nm, max. 1.8 W) was focused onto the Yb:Nb:RTP sample by a 6.28 cm lens L to a Gaussian waist of $\approx 30 \mu\text{m}$. The ≈ 150 cm long astigmatically compensated cavity consisted of two folding mirrors (M1 and M2), both with a radius of curvature equal to -10 cm, a rear plane mirror, M3, and the plane output coupler, M4, with transmission of 1% or 3%.

The Yb:Nb:RTP sample used (Fig. 1) had dimensions of ≈ 3 mm along the a - and c -axes, and ≈ 2.5 mm along the b -axis, and four of its faces ($\perp a$ and $\perp b$) were polished. The Yb-density in the crystal, measured by EPMA, was $1.9 \times 10^{20} \text{ cm}^{-3}$. The sample was inserted under Brewster angle between the two folding mirrors and no special cooling was applied.

The input-output characteristics of the Yb:Nb:RTP laser are summarized in Fig. 3 for the three possible polarizations and propagation along the a -axis (a) and b -axis (b). The pump wavelength was 972.1 nm ($E\parallel a$ and $E\parallel c$) and 972.7 nm ($E\parallel b$). In all cases the pump spectral width was much narrower than the FWHM of the corresponding absorption lines (3.6, 4.1, and 3.7 nm for polarization parallel to the a , b , and c -axes, respectively).

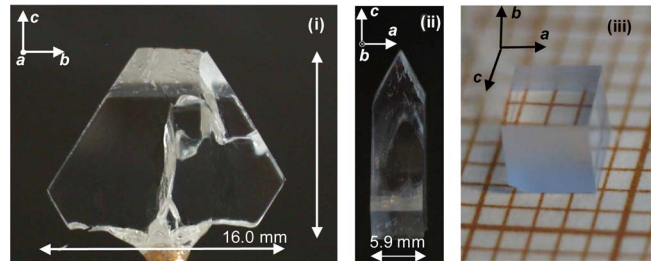


Fig. 1. (Color online) Yb:Nb:RTP crystal grown by the TSSG-SC method with a c -oriented seed (i, ii) and sample used in the laser study (iii).

The highest absorption cross-section is for $E\parallel b$ (see [8]) with maximum absorption for propagation along the a -axis. In this case, a maximum output power of 154 mW at 1050.6 nm was obtained using an output coupler with $T=1\%$, for an absorbed pump power of 386 mW. The corresponding slope efficiency was $\eta=42.5\%$. and the threshold (absorbed power) was $P_{th}=35$ mW.

The performance of the laser for $E\parallel c$ and propagation direction along the a - and b - axes was very similar although the sample thickness was different. For propagation along the b -axis, the slope efficiency reached $\eta=60.1\%$ for $T=3\%$, while propagation along the a -axis resulted in an output power of 115 mW with $T=1\%$, for an absorbed pump power of 323 mW.

For $E\parallel a$ and propagation along the b -axis, generation was obtained only in the case $T=1\%$ and the slope efficiency was lower compared to $E\parallel b$ and $E\parallel c$, presumably because of the smaller gain cross-section.

The laser wavelength was basically the same for the three polarizations and the two output couplers, i.e., the maximum of the gain curve remains unchanged. The extremely low laser thresholds are related to the large splitting of the ground state.

With lasing interrupted, the absorption of the sample was bleached at the maximum incident pump power of 1.8 W. Under lasing conditions the absorption was still quite low (13% for $E\parallel a$, 25-20% for $E\parallel b$, and 15%-20% for $E\parallel c$ depending on the output coupler used) and remained almost constant with in-

Table 1. Yb:Nb:RTP Single Crystal Growth

Exp.	T_S [K]	Seed Dimensions ($x \times y \times z$) [mm]	Axial Gradient [K/cm]	Cooling Range [K]	Cooling Ramp [K/h]	Crystal Dimensions ($x \times y \times z$) [mm]	Crystal Weight [g]
1	1195.5	$3.65 \times 1.5 \times 5$	2	0.1	1	$4.97 \times 14.40 \times 11.80$	1.8148
				4	0.05		
				9	0.02		
2	1195.0	$4.77 \times 1.5 \times 5$	2	0.1	1	$5.46 \times 13.99 \times 11.46$	1.9945
				4	0.05		
				9	0.02		
3	1187.0	$4.90 \times 1.5 \times 5$	2.4	1	1	$5.28 \times 12.53 \times 11.18$	1.5172
				6	0.05		
				7.5	0.03		
4	1187.5	$5.20 \times 1.5 \times 5$	2.4	1	1	$5.95 \times 16.04 \times 12.69$	2.6029
				6	0.05		
				10	0.03		

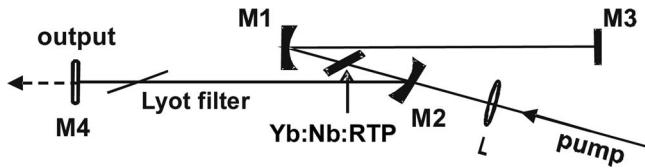


Fig. 2. Experimental setup of the Yb:Nb:RTP laser.

172 creasing pump power. This is a consequence of the
 173 low Yb-ion density in the crystal and the relatively
 174 low absorption cross-sections. However, in the lasing
 175 state, the intracavity power in the three-level Yb-
 176 system increases the pump saturation intensity, and
 177 this balances the bleaching effect.
 178 The tuning behavior of the laser was studied in-
 179 serting a birefringent filter in the vicinity of the out-
 180 put coupler, Fig. 4. The obtained linewidth was below
 181 our resolution of 0.5 nm. The broadest tuning range
 182 was obtained for $E//b$ although all three curves look
 183 quite similar. The FWHM is 59 nm, which is an indi-
 184 cation of the potential of Yb:Nb:RTP for generation
 185 of ultrashort (femtosecond) laser pulses. Such a
 186 broad tuning range and the relatively low wave-
 187 lengths that were obtained are also related to the

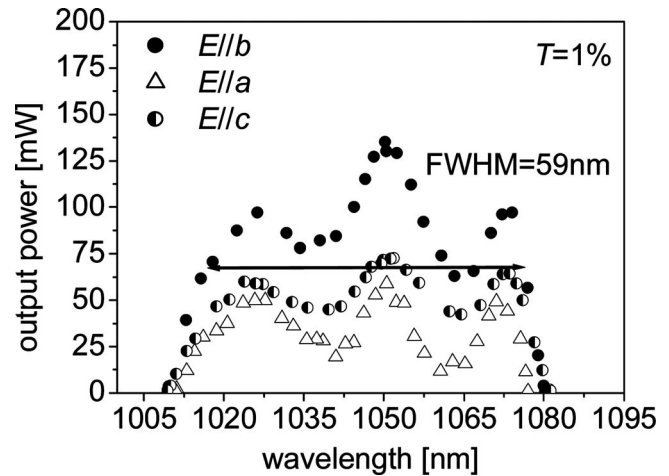


Fig. 4. Wavelength tunability of the Yb:Nb:RTP laser with a two-plate intracavity Lyot filter for the three polarizations. In the case of $E//c$ the propagation is along the a -axis.

188 large splitting of the ground state: the three peaks in
 189 Fig. 4 correspond to transitions from the two lowest
 190 sublevels of the upper multiplet to the two highest
 191 sublevels of the lower multiplet [8].

192 We experimentally determined the fundamental
 193 wavelength for noncritical type-II second harmonic
 194 generation and obtained 1120 and 985 nm for the
 195 propagation along the a and b axes, respectively.
 196 These results are very similar to those published for
 197 Nb:RTP [10]. Since the laser wavelength found for
 198 Yb:Nb:RTP is within the above range, in principle
 199 SFD operation should be possible at some interme-
 200 diate propagation direction in the a - b plane. Work is
 201 in progress to achieve this.

202 In conclusion, we achieved continuous-wave laser
 203 operation of Yb at room temperature in orthorhombic
 204 Nb:RTP around 1050 nm for all three possible polar-
 205 izations, which guarantees that this also will be possi-
 206 ble along any phase-matching direction of second
 207 harmonic generation. This should be confirmed in
 208 further experiments. The tuning range extended
 209 from 1009 to 1081 nm. We are confident that a fur-
 210 ther increase of the doping level could drastically im-
 211 prove these initial laser results with Yb:Nb:RTP in
 212 terms of output power. Diode-pumping and further
 213 power scaling should also be possible, having in mind
 214 the broad absorption spectrum of Yb:Nb:RTP. The
 215 extremely broad tunability achieved is also promis-
 216 ing for mode-locking to obtain femtosecond pulses
 217 and self-frequency conversion with this material.

218 This work was supported through the European
 219 Union project DT-CRYS, NMP3-CT-2003-505580, and
 220 by the Catalan government by Project 2005SGR658
 221 and the Ministerio de Educación y Ciencia of the
 222 Spanish government, under Projects MAT-05-06354-
 223 C03-02, MAT-04-20471-E, and CIT-020400-2005-14.

224 **References**

225 1. A. Brenier, *J. Lumin.* **91**, 121 (2000).
 226 2. P. Dekker, P. A. Burns, J. M. Dawes, and J. A. Piper, *J.*
 227 *Opt. Soc. Am. B* **20**, 706 (2003).

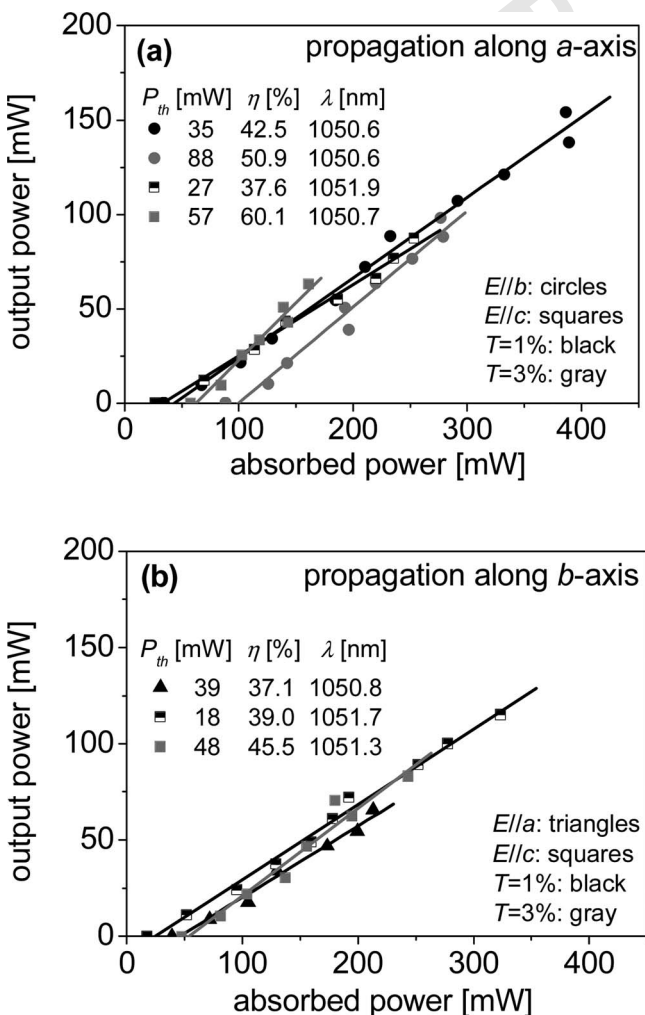


Fig. 3. Input-output characteristics of the Yb:Nb:RTP laser for different output coupling (T) and polarization (E): P_{th} : threshold absorbed power, η : slope efficiency, λ : oscillation wavelength.

- 228 3. Z. Zhu, J. Li, B. Alain, G. Jia, Z. You, X. Lu, B. Wu, and
229 C. Tu, *Appl. Phys. B* **86**, 71 (2007).
230 4. A. Aron, G. Aka, B. Viana, A. Kahn-Harari, D. Vivien,
231 F. Druon, F. Balembois, P. Georges, A. Brun, N. Lenain,
232 and M. Jaquet, *Opt. Mater.* **16**, 181 (2001).
233 5. H. Zhang, X. Meng, P. Wang, L. Zhu, X. S. Liu, X. M.
234 Liu, Y. Yang, R. Wang, J. Dawes, J. A. Pipper, S.
235 Zhang, and L. Sun, *J. Cryst. Growth* **222**, 209 (2001).
236 6. L. E. Bausá, M. O. Ramírez, and E. Montoya, *Phys.*
237 *Status Solidi A* **201**, 289 (2004).
238 7. I. Parreu, M. C. Pujol, M. Aguiló, F. Díaz, X. Mateos,
and V. Petrov, *Opt. Express* **15**, 2360 (2007). 239
8. J. J. Carvajal, R. Sole, Jna. Gavalda, J. Massons, P. 240
Segonds, B. Boulanger, A. Brenier, G. Boulon, J. 241
Zaccaro, M. Aguiló, and F. Diaz, *Opt. Mater.* **26**, 313 242
(2004). 243
9. J. J. Carvajal, V. Nikolov, R. Solé, Jna. Gavalda, J. 244
Massons, M. Rico, C. Zaldo, M. Aguiló, and F. Díaz, 245
Chem. Mater. **12**, 3171 (2000). 246
10. J. J. Carvajal, P. Segonds, A. Peña, J. Zaccaro, B. 247
Boulanger, F. Díaz, and M. Aguiló, *J. Phys. Condens.* 248
Matter **19**, 116214 (2007). 249

PROOF COPY [80195] 516714OPL

#1 AQ: Please verify all grammar edits

PROOF COPY [80195] 516714OPL